Tuneable Peak Deformations in Chiral Liquid Chromatography

ARTICLE *in* ANALYTICAL CHEMISTRY · SEPTEMBER 2007

Impact Factor: 5.64 · DOI: 10.1021/ac062330t · Source: PubMed

3 AUTHORS, INCLUDING:

Patrik Forssén
Karlstads universitet
30 PUBLICATIONS **415** CITATIONS
SEE PROFILE

Torgny Fornstedt
Karlstads universitet
105 PUBLICATIONS **1,794** CITATIONS
SEE PROFILE

Anal. Chem. **2007,** *79,* 5838−5847

Tuneable Peak Deformations in Chiral Liquid Chromatography

Robert Arnell, Patrik Forssén, and Torgny Fornstedt*

Department of Physical and Analytical Chemistry, Uppsala University, BMC Box 577, SE-751 23, Uppsala, Sweden

Modern chiral stationary phases are often combined with eluents comprising a mixture of organic solvents and polar additives. The latter may cause extreme deformations of the eluted enantiomer bands in both analytical and preparative separations. In this work, we give a theoretical background for these deformations. As an experimental verification, we separate the enantiomers of different *β*-blockers on a teicoplanin stationary phase (Chirobiotic T) in the presence of triethylamine/acetic acid. We show that it is possible to tune the peak shapes of the two enantiomers by varying the organic solvent composition. An advantageous situation occurs when the first eluted peak is transformed to an anti-Langmuirian shape while keeping the second enantiomer in a normal Langmuirian shape. In this situation, the two peaks tail in opposite directions with their sharp sides pointing closely to each other. It is then possible to obtain baseline resolution at higher load than when both enantiomer peaks tail in the same direction. Adsorption isotherm parameters were determined using the inverse method; no other method could be used due to the system complexity. Computer simulations, based on these parameters, agreed very well with the observed deformations, thus confirming our hypothesis of their origin.

The FDA's policy statement for the development of new stereoisomeric drugs,[1] published in 1993, required the evaluation of pharmacologic and pharmacokinetic activities on each single enantiomer at an early stage of drug development. Because of the thousands of drug candidates at this stage, it is essential with fast methods for purification of milligram−gram amounts of enantiomers. This has triggered the development of many new chiral stationary phases (CSPs) with high selectivities, capacities, and efficiencies. At the high sample load applied on these modern columns, enantiomer peaks sometimes become extremely deformed, which has a negative impact on the separation. This study is a contribution to the understanding of the causes of such deformations.

Much research has been done to understand the fundamentals of chromatography. Various mathematical models have been formulated, describing the migration, adsorption, and mass transfers inside the chromatography column.[2−5] With the development of computational science, it has become possible to use increasingly complex and realistic models in the analysis. The models are complex due to the fact that the different solutes compete for a limited number of adsorption sites; the adsorbed concentration of any solute therefore depends on the local concentration of all solutes. This equilibrium is described by competitive adsorption isotherms, which are central in any chromatographic model since they determine the peak shapes.[5]

Type-I adsorption isotherms have convex curvature and are the most common ones. At overload they give rise to tailing "Langmuirian" peaks with a steep front and diffuse rear since the high-concentration region in the band migrates faster than the low-concentration region does. The simplest models, like the Langmuir isotherm, assume a homogeneous surface, ideal solutions, and monolayer capacity.[5] Surface heterogeneity is often accounted for by multiple Langmuirian terms.[6] Type-III adsorption isotherms have concave curvature and are much less common; they give rise to leading "anti-Langmuirian" peaks with diffuse front and steep rear. In between are the type-II, "S-shaped", adsorption isotherms with an inflection point, giving rise to a mixed Langmuirian and anti-Langmuirian behavior. Several models accounting for "strange", non-Langmuirian peaks have been proposed, for instance, the quadratic model,[5] and the models by Brunauer−Emmet−Teller,[7] Moreau,[8] and Szabelski.[9] The adsorption of Tröger's base on Chiralpak AD is very good example of this.[10] These models are all very complex and contain many parameters.

Surprisingly, non-Langmuirian peaks can also occur in LC systems where all components are governed by type-I adsorption isotherms. If adsorbing additives are used in the eluent, the peaks may have anti-Langmuirian appearance, be split, or show strange forms that are normally not associated with convex models. A

* To whom correspondence should be addressed. E-mail: torgny.fornstedt@ytbiotrknik.uu.se.

(1) FDA's Policy Statement for the Development of New Stereoisomeric Drugs. http://www.fda.gov/cder/guidance/stereo.htm. 5 Jan 1993.

(2) Wilson, J. N. *J. Am. Chem. Soc.* **1940**, *62*, 1583−1591.

(3) Giddings, J. C. *Dynamics of Chromatography*; M. Dekker: New York, 1965.

(4) Helfferich, F.; Klein, G. *Multicomponent Chromatography*; M. Dekker: New York, 1970.

(5) Guiochon, G.; Felinger, A.; Shirazi, D. G.; Katti, A. K. *Fundamentals of Preparative and Nonlinear Chromatography*, 2nd ed.; Elsevier Inc.: San Diego, CA, 2006.

(6) Jacobson, S.; Golshan-Shirazi, S.; Guiochon, G. *J. Am. Chem. Soc.* **1990**, *112*, 6492−6498.

(7) Brunauer, S.; Emmet, P. H.; Teller, J. *J. Am. Chem. Soc.* **1938**, *60*, 309−319.

(8) Moreau, M.; Valentin, P.; Vidal-Madjar, C.; Lin, B., C.; Guiochon, G. *J. Colloid Interface Sc.* **1991**, *141*, 127−136.

(9) Szabelski, P.; Kaczmarski, K. *J. Chromatogr., A* **2006**, *1113*, 74−83.

(10) Mihlbachler, K.; Kaczmarski, K.; Seidel-Morgenstern, A.; Guiochon, G. *J. Chromatogr., A* **2002**, *955*, 35−52.

10.1021/ac062330t CCC: $37.00
Published on Web 06/23/2007

prerequisite for the occurrence of such distortions is that the additive be more strongly retained than the solute in the pure weak solvent.[11,12] It was found that the most amazing and strange type of band shapes could take place at large sample loads depending on the additive concentration and sample size.[11,12] However, Fornstedt and Guiochon later developed a rule of thumb for when the most important classes of band shapes appear.[13,14] We will return to this issue in the Theory section.

Modeling of chiral separations is challenging since the interactions are complex and the exact retention mechanism is not always known. When non-Langmuirian peaks are encountered, the classical explanation is that the solutes are governed by non-Langmuirian adsorption isotherms (type-II or type-III). We believe that the peak deformations in many modern chiral systems are due to the effects caused by strongly adsorbed additives.[11−14] In the present study, we will show that this theory applies to the chiral separation of β-blockers on an immobilized teicoplanin stationary phase (Chirobiotic T) when typical methanol/acetonitrile eluents with acetic acid/triethylamine additives are used. Detailed characterization by adsorption isotherm determination has been impossible with traditional methods, such as frontal analysis,[5] because of the extraordinary system complexity. We will also show that the inverse method (IM),[15−18] developed in recent years, is a powerful tool for characterization of modern chiral LC systems. We will use the IM to measure both β-blocker and additive adsorption and use computer simulations to confirm our hypothesis. More particularly, the aims of this study are to (i) prove that the effects can take place in a modern chiral system, intended for preparative separations, by using the IM as tool and to (ii) demonstrate how the effects can be controlled.

THEORY

Column Model. The equilibrium-dispersive model[5] was used to describe the migration of solute concentrations, C_i, through the LC column, with one partial differential mass balance equation per component. In this study, there were three components, *R*- and *S*-enantiomers and the additive, so $\mathbf{C} = (C_R, C_S, C_a)$. The column was equilibrated with an eluent containing an additive concentration $C_{p,a}$ (index p indicates that it is a plateau concentration), so the initial conditions were $\mathbf{C}(x, 0) = (0, 0, C_{p,a})$. The boundary condition was the concentration profile of the injected sample at the column inlet. The elution profile was calculated by solving the mass balance equations using a modified Rouchon method as described elsewhere.[18]

Adsorption Isotherm Models. In the theoretical introduction to additive perturbations and solute peak deformations below, all examples are for simplicity based on the Langmuir adsorption isotherm

$$q_i(\mathbf{C}) = \frac{a_i C_i}{1 + \sum_j b_j C_j} \tag{1}$$

where q_i is the adsorbed concentration of component i, a is the initial slope of the adsorption isotherm, and b is the equilibrium constant.

When fitting to experimental data, we instead used the heterogeneous competitive bi-Langmuir adsorption isotherm model[6] to describe the equilibrium between mobile and stationary phases:

$$q_i(\mathbf{C}) = \frac{a_{\mathrm{I},i} C_i}{1 + \sum_j b_{\mathrm{I},j} C_j} + \frac{a_{\mathrm{II},i} C_i}{1 + \sum_j b_{\mathrm{II},j} C_j} \tag{2}$$

The first Langmuirian term describes nonchiral binding, and the second Langmuirian term describes chiral binding.

Additive Perturbations and Solute Peak Deformations. If an eluent containing an adsorbing additive, with concentration $C_{p,a}$, is pumped through an LC column, a concentration $q_a(C_{p,a})$ will be adsorbed throughout the column once equilibrium has been reached. If a sample with a composition different from that of the eluent is injected, there will be a perturbation of the additive equilibrium. Displaced additive will then propagate like a fast-moving wave through the column. If the additive can be detected, the perturbation will be visualized as the perturbation peak (also called system peak).[5] The retention time of the perturbation peak is proportional to the tangential slope of the adsorption isotherm at the actual additive bulk concentration in the eluent (eqs 4 and 5, below). Further additive disturbances will, due to the coherence condition,[4] coelute with and give positive or negative contributions to each solute peak. If the injected sample concentration deviates only slightly from $C_{p,a}$ and the injected solute concentrations are low, the resulting peaks will be Gaussian. The retention times of the solutes ($t_{R,i}$) and the additive perturbation peak ($t_{R,a}$) will be

$$t_{\mathrm{R},i} = t_0\left(1 + F\frac{\partial q_i}{\partial C_i}\bigg|_{C_a = C_{p,a}, C_i = 0}\right) \tag{3}$$

$$t_{\mathrm{R,a}} = t_0\left(1 + F\frac{\partial q_a}{\partial C_a}\bigg|_{C_a = C_{p,a}}\right) \tag{4}$$

where t_0 is the column holdup time and F is the phase ratio. The retention times of solutes and the perturbation are strongly dependent on the additive plateau concentration. In the case of the Langmuir adsorption isotherm, the retention times will be

$$t_{\mathrm{R},i} = t_0\left(1 + F\frac{a_i}{1 + b_a C_{p,a}}\right) \tag{5}$$

$$t_{\mathrm{R,a}} = t_0\left(1 + F\frac{a_a}{(1 + b_a C_{p,a})^2}\right) \tag{6}$$

In previous publications,[13,14] it was demonstrated that very strange solute band shapes may occur when the additive component has stronger adsorption strength than the solute. Under such conditions, the additive peak has a larger capacity ratio (also called

(11) Golshan-Shirazi, S.; Guiochon, G. *Anal. Chem.* **1989**, *61*, 2373−2380.
(12) Golshan-Shirazi, S.; Guiochon, G. *Anal. Chem.* **1989**, *61*, 2380−2388.
(13) Fornstedt, T.; Guiochon, G. *Anal. Chem.* **1994**, *66*, 2116−2128.
(14) Fornstedt, T.; Guiochon, G. *Anal. Chem.* **1994**, *66*, 2686−2693.
(15) James, F.; Sepúlveda, M.; Charton, F.; Quiñones, I.; Guiochon, G. *Chem. Eng. Sci.* **1999**, *54*, 1677−1696.
(16) Felinger, A.; Cavazzini, A.; Guiochon, G. *J. Chromatogr., A* **2003**, *986*, 207−225.
(17) Arnell, R.; Forssén, P.; Fornstedt, T. *J. Chromatogr., A* **2005**, *1099*, 167−174.
(18) Forssén, P.; Arnell, R.; Fornstedt, T. *Comp. Chem. Eng.* **2006**, *30*, 1381−1391.

retention factor) than the solute if these components are both injected as solutes into a column lacking the additive, i.e., containing only the pure weak solvent. Now, if the column instead is equilibrated with a constant stream of additive and if a small excess or deficiency of additive molecules is injected into the column, a perturbation peak appears (if the additive signal can be detected). Depending on the relative retention of the additive perturbation peak and the solute peak at infinitesimal sample sizes but finite additive concentrations in the mobile phase, the solute peak may take a very different shape at large sample loads. A rule of thumb[13,14] will be given below describing when Langmuirian or anti-Langmuirian peaks will arise.

The solute peak is shaped during the migration through additive concentration gradients in the displaced zones, just as the displaced additive zones are shaped by the concentration gradients of the solute peak. This complicated cause-and-effect problem has been extensively studied previously,[13,14] where it was shown under which circumstances Langmuirian solutes peaks can be inverted to anti-Langmuirian peaks (although the isotherm is still Langmuirian). The rule of thumb was developed in this context to provide simpler means to analyze complex multicomponent systems and it will be extensively used in the present study.

If a small sample of additive and solute molecules is separated on a column equilibrated with additive-free eluent, i.e., $C_{p,a} = 0$, the elution order of the injected solute and additive molecules is given by

$$t_{R,i} = t_0(1 + Fa_i|_{C_{p,a}=0}) \quad (7)$$

assuming the Langmuir model. The selectivity $\alpha_{0,i}$ will be

$$\alpha_{0,i} = \frac{k_a}{k_i}|_{C_{p,a}=0} = \frac{t_{R,a} - t_0}{t_{R,i} - t_0}|_{C_{p,a}=0} = \frac{dq_a/dC_a}{dq_i/dC_i}|_{C_a,C_i\to 0} \quad (8)$$

where k_j is the capacity ratio of component j. If the initial slope of the additive adsorption isotherm is less steep than that of a solute, that is, $\alpha_{0,i} < 1$, then solute i will always be Langmuirian at overload for any $C_{p,a}$. If, on the other hand, the initial slope of the additive adsorption isotherm is steeper than that of the solute, or equivalently, $\alpha_{0,i} > 1$, then the solute peak may display non-Langmuirian characteristics at overload when $C_{p,a} \neq 0$. The outcome is given by the elution order of small solute (eq 3) and additive perturbation (eq 4) peaks, which is dictated by $C_{p,a}$, the additive concentration of the eluent. The selectivity on an additive concentration plateau, $\alpha_{p,i}$, is expressed as

$$\alpha_{p,i} = \frac{k_{p,a}}{k_{p,i}}|_{C_a=C_{p,a}} = \frac{t_{R,a} - t_0}{t_{R,i} - t_0}|_{C_a=C_{p,a}} \quad (9)$$

Notice that in eq 8 $t_{R,a}$ is the retention time of the injected additive sample, whereas in eq 9 it is the retention time of the additive perturbation peak, which are not equivalent.[19] All retention times in eq 9 are measured in the presence of a competing additive, so the k_p values are only *apparent* capacity ratios. If $\alpha_{0,i} > 1$ and the perturbation peak elutes after the solute does ($\alpha_{p,i} > 1$), the overloaded solute peak will be Langmuirian. If the elution order is reversed ($\alpha_{p,i} < 1$), then the overloaded solute peak will have an anti-Langmuirian appearance. Finally, if the additive perturbation and solute peaks are poorly separated ($\alpha_{p,i} \approx 1$), complex solute peak deformations occur. The reason why the additive peak can elute before the solute peak ($\alpha_{p,i} < 1$) although the adsorption strength of the additive is larger ($\alpha_{0,i} > 1$) is understood by comparing eqs 5 and 6. When the bulk concentration of the additive is increased ($C_{p,a}$) the retention time of the additive perturbation peak decreases faster than that of the solute. It is crucial at this point to understand that varying the additive concentration in the eluent ideally cannot affect $\alpha_{0,i}$, only $\alpha_{p,i}$. This is because $\alpha_{0,i}$ correspond to the adsorption when using the weak eluent lacking additive. Obviously $\alpha_{0,i}$ depend on the properties of the weak eluent, so the choice of weak eluent composition should be very important in this context. This will be studied and exploited in the present study.

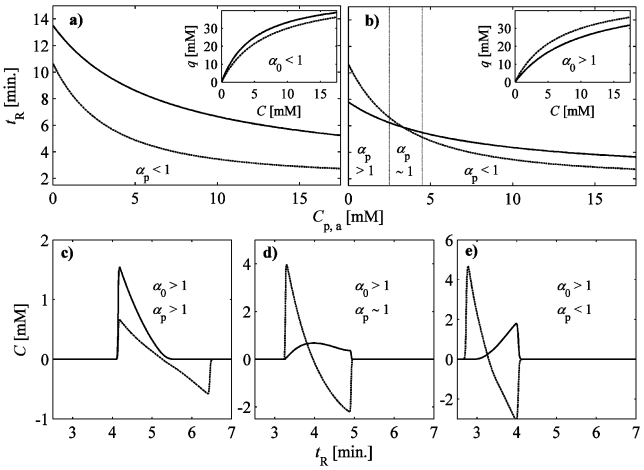

Figure 1. Visualization of additive effects on the solute peak shape. The retention times of the solute (solid) and perturbation peak (dashed) for different additive concentrations ($C_{p,a}$) in the eluent; (a) weakly adsorbed additive, (b) strongly adsorbed additive. Inset: adsorption isotherms. In case a, the solute peak will always be Langmuirian (not shown). In case b, the solute peak shape depends on the elution order of the solute and perturbation peaks, which in turn depends on $C_{p,a}$. For an eluent with $C_{p,a} = 1$ mM (c) the solute peak is Langmuirian, at 4 mM (d) oddly deformed, and at 8 mM (e) it is anti-Langmuirian.

This rule of thumb is visualized by simulations in Figure 1, where it is shown how the initial slopes of the adsorption isotherms and the relative elution order affect the shape of an overloaded solute peak. It should be noted that the overloaded perturbation is always Langmuirian, whereas the coherent disturbance and solute peak may take a wide array of shapes. Many detectors have low sensitivity for additives, so in most situations, only the solute contribution is seen in the chromatogram.

EXPERIMENTAL SECTION

Apparatus. An Agilent 1100 chromatography system (Agilent Technologies, Palo Alto, CA) was used, consisting of binary pump, autosampler, and diode array UV detector modules and acquisition software. A Beckman 156 refractive index (RI) detector was connected after the UV detector. Column temperature was controlled by a Lauda B pump thermostat (Lauda, Königshofen,

(19) Samuelsson, J.; Forssén, P.; Stefansson, M.; Fornstedt, T. *Anal. Chem.* **2004**, *76*, 953−958.

Germany) by circulating water through the column compartment. PEEK capillaries (i.d. 0.13 mm) and a 0.5-μm precolumn filter (Upchurch Scientific Inc., Oak Harbor, WA) were used. An Advantec SF-2100W fraction collector (Toyo Roshi, Dublin, CA) and an Orion 9126 pH electrode (Thermo Orion, Beverly, MA) were used. A Chirobiotic T column (Advanced Technologies Inc., Whippany, NY), length 250 mm, i.d. 4.6 mm,and particle size 5 μm was used. The column efficiency was 11 250 theoretical plates (N), measured from analytical β-blocker peaks.

Chemicals. Racemic alprenolol and propranolol hydrochlorides and propranolol hydrochloride enantiomers (>99% purity) were obtained from Sigma-Aldrich. (*R*)-Alprenolol tartrate monohydrate, (*S*)-alprenolol phosphate, and racemic atenolol (>99% purity) were kind gifts from AstraZeneca (Mölndal, Sweden). All eluent components—methanol (MeOH), acetonitrile (ACN), acetic acid (HOAc), and triethylamine (TEA)—were of HPLC grade and from Sigma-Aldrich. All eluent compositions are given as volumetric ratios. Eluents were degassed by ultrasonication prior to use. Water was delivered by a MilliQ Academic unit (Millipore, Molsheim, France).

Procedures. Experiments were performed at 25 ± 0.1 °C with 1.50 mL min^{-1} flow rate. Analytical peaks (50 μM of each enantiomer) were detected at 270 nm. Overloaded peaks (up to 50 mM of each enantiomer) were detected at 290 (alprenolol and atenolol) and 330 nm (propranolol). The additive perturbation peak was detected by RI and could often but not always also be seen on UV at 214 nm. All injected samples were, unless stated otherwise, dissolved in eluent. For each eluent composition, the column holdup time was estimated from the first disturbance seen on RI.

The IM was used to estimate the competitive adsorption isotherms of additive and β-blockers for two eluents. We used the following version of the bi-Langmuir adsorption isotherm model in eq 2:

$$q_i(\mathbf{C}) = \frac{a_{\mathrm{I},i}C_i}{1 + b_{\mathrm{I,a}}C_{\mathrm{a}} + b_{\mathrm{I},RS}(C_R + C_S)} + \frac{a_{\mathrm{II},i}C_i}{1 + \sum_j b_{\mathrm{II},j}C_j} \quad (10)$$

The *R*- and *S*-isomers have common a_{I} and b_{I} parameter values, but the additive may have a different affinity for the nonchiral binding site. The *R*- and *S*-isomers and the additive have unique a_{II} and b_{II} parameter values for the chiral binding site.

In the IM, adsorption isotherm parameters are fitted to experimental elution profiles. The chromatographic process is numerically simulated using a starting guess of the adsorption isotherm parameters. The elution profiles are calculated iteratively, and the adsorption isotherm model parameters are adjusted until the calculated chromatograms coincide with experimental ones. The parameters, corresponding to a chosen adsorption isotherm model that best describe the adsorption system, are thus obtained. The β-blockers were analyzed separately as racemic mixtures. The column was equilibrated with an eluent containing additive, and three 50-μL injections were performed for each β-blocker: 5, 25, and 50 mM (sum of enantiomer concentrations). Adsorption isotherm parameters were fit to the 3 × 3 resulting chromatograms using an IM algorithm described elsewhere.[18] The additive adsorption isotherm parameters were determined indirectly from the shapes of the β-blocker peaks; no fitting was done directly to additive perturbation peaks.

UV detector calibration was performed at relevant wavelengths to find the relation between the nonlinear detector response and concentrations. The column was temporarily displaced, and samples containing known β-blocker concentrations (dissolved in eluent) were pumped through the detector. Each calibration curve was constructed from 20 data points. The accuracy of IM may be increased if the injection profile is recorded experimentally and then used in the calculations.[15] The injection profiles corresponding to 50- and 500-μL samples were measured by displacing the column and injecting a low concentration directly into the detector. Long PEEK capillaries (i.d. 0.13 mm) were then temporarily connected before the injector and after the detector in order to maintain high-pressure operating conditions.

Safety. Most eluent components used are volatile and toxic. The pharmaceutical compounds used have strong physiological effects.

RESULTS AND DISCUSSION

Macrocyclic glycopeptide antibiotics, covalently immobilized to silica, is a very useful new class of CSPs for enantioseparations in HPLC.[20,21] Among these, the CSP based on teicoplanin (Chirobiotic T, Astec) has shown great versatility in both reversed-phase and normal-phase mobile phases. Teicoplanin contains a heptapeptide aglycon with seven aromatic rings, four phenolic groups, six amido groups, three ether links, and two chlorine atoms. A more detailed description is found in ref 21. The CSP was able to resolve all naturally occurring amino acids in their native form with methanol/water as mobile phase.[20] Other compounds, such as β-blockers, are best separated in the polar organic mode using eluents of intermediate polarity. In this study, we used such eluents, MeOH/ACN mixtures containing a HOAc/TEA ratio as additives, recommended by the column manufacturer. In the initial stage of this research, we found that β-blocker elution profiles could take the most fascinating shapes, depending on the eluent composition. Figure 2 shows the elution profiles obtained with a MeOH/ACN/HOAc/TEA 67.3/32.5/0.15/0.05 eluent and 50 μL of 50 mM samples. The alprenolol enantiomers (a) elute before the propranolol enantiomers (b), which in turn elute before the atenolol enantiomers (c). Most interestingly, the alprenolol peaks are anti-Langmuirian; the first propranolol peak (*S*) is anti-Langmuirian whereas the second one (*R*) is Langmuirian; finally, both atenolol peaks are Langmuirian. Injection of single enantiomers of alprenolol and propranolol showed that the (*S*)-forms elute before the (*R*)-forms (not shown). This analysis could not be repeated for atenolol since no pure enantiomers were available, but we assume that the same elution order holds for atenolol. At a first glance, it seems like the remarkable peak shapes in Figure 2 depend on the retention time and that there is a symmetry shift at ~14 min, i.e., in between the propranolol peaks. Solutes eluting before this point are anti-Langmuirian, whereas those eluting after have Langmuirian shape.

The resolution is highest by far in the propranolol case, where the peaks tail in opposite directions; almost baseline resolution is

(20) Berthod, A.; Liu, Y.; Bagvill, C.; Armstrong, D. W. *J. Chromatogr., A* **1996**, *731*, 123−137.
(21) Berthod, A.; Valleix, A.; Tizon, V.; Leonce, E.; Caussignac, C.; Armstrong, D. W. *Anal. Chem.* **2001**, *73*, 5499−5508.

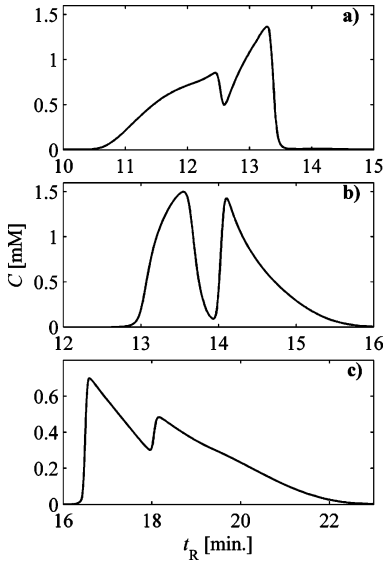

Figure 2. 50 μL of 50 mM (a) alprenolol, (b) propranolol, (c) and atenolol (dissolved in eluent) separated on a Chirobiotic T column, eluent MeOH/ACN/HOAc/TEA 67.3/32.5/0.15/0.05. The peaks have fundamentally different shapes, although identical experimental conditions were used.

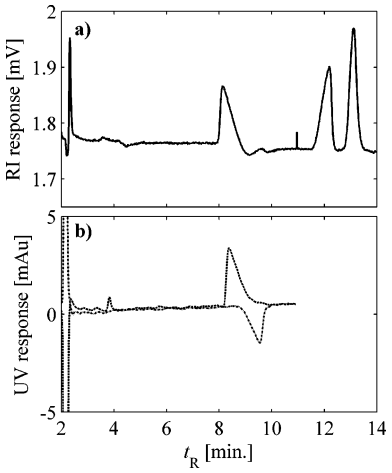

Figure 3. Analysis of adsorbed eluent components. Eluent: MeOH/ACN/HOAc/TEA 67.3/32.5/0.15/0.05. (a) RI trace of a 50 μL of 10 mM alprenolol (dissolved in eluent) sample injection. (b) Additive perturbations monitored with UV detector at 214 nm; injection of a 50-μL solution containing an excess of TEA, MeOH/ACN/HOAc/TEA 67.4/32.5/0/0.1 (dashed line) and of a solution lacking TEA, 67.3/32.5/0.18/0 (dash−dotted line).

achieved. The resolution is far worse in the alprenolol and atenolol cases. This pattern with opposite tailing should therefore be very desirable in a preparative separation.

The profiles in Figure 2 might suggest that some components are governed by type-I adsorption isotherms whereas others are governed by type-III adsorption isotherms. This would suggest a strongly cooperative binding of weakly retained components only, which seems unlikely. A more likely explanation of the symmetry shift is that it is an effect caused by a strongly adsorbed additive. In the following sections, we investigate whether this hypothesis is valid.

Identification of the Strongly Adsorbed Additive. An RI detector connected to the column outlet revealed an additional peak, eluted before all β-blocker enantiomer peaks. The retention time of this extra peak was the same regardless of the sample (for instance, pure methanol), suggesting it to be a perturbation peak. Figure 3a shows the RI signal corresponding to a 50-μL 10 mM alprenolol sample injection (solute dissolved in eluent); the perturbation elutes before the two enantiomer peaks. This perturbation peak corresponds to an adsorbing eluent component—MeOH, ACN, HOAc, or TEA. The first two were ruled out by equilibrating the column with a MeOH/ACN 67.5/32.5 eluent and perturbing the system by injecting different rations of MeOH/ACN; the only peaks observed eluted near t_0 (the column holdup time), implying that the adsorption of MeOH and ACN is negligible. Next, the column was equilibrated with the original eluent, MeOH/ACN/HOAc/TEA 67.3/32.5/0.15/0.05. The UV signals at 214 nm corresponding to two 50-μL perturbation injections are shown in Figure 3b. The first sample (dashed) consisted of MeOH/ACN/HOAc/TEA 67.4/32.5/0/0.1, introducing a negative HOAc and a positive TEA perturbation. This resulted in a negative peak at t_0 and a positive peak with the same retention time as the perturbation peak in Figure 3a. The second sample (dash−dotted) consisted of MeOH/ACN/HOAc/TEA 67.3/32.5/0.18/0, introducing a positive HOAc and a negative TEA perturbation. This resulted in a positive peak at t_0 and a negative peak with the same limit retention time as the positive dashed perturbation peak (the limit retention time of overloaded positive and negative perturbation peaks is described elsewhere[22]). From this we concluded that TEA is the only adsorbing component, and it should thus be the additive to account for in eq 2 and the key factor in the symmetry shift observed in Figure 2.

Eluent Screening. After the identification of the adsorbing additive, an extensive eluent screening was performed. The eluent composition was varied to get insight into how TEA and the other eluent components affect retention times of perturbation and β-blocker peaks and also β-blocker peak symmetries. For measurement of analytical retention times, 0.10 mM racemic samples were injected; 0.50 mM samples were, however, used when the retention times were extremely long. For the study of overloaded peaks, we choose to inject 5.0 mM racemic mixtures. With this concentration, system nonlinearity was strong enough for overload, while the peak widths were kept relatively small. This way we avoided the risk of having overloaded peaks extend into zones with different characteristics. For convenience, we used the peak symmetry factor as calculated by the Agilent Chemstation software, based on a pseudomoment analysis. For Langmuirian peaks with a steep front and diffuse rear, the symmetry factor is below unity, anti-Langmuirian peaks have a symmetry factor exceeding unity, and Gaussian peaks have symmetry equal to one. Oddly deformed peaks that exhibit partially Langmuirian and partially anti-Langmuirian characteristics often have a symmetry factor close to unity.

The effects of the total concentration of additive, keeping the HOAc/TEA additive ratio constant, are depicted in Figure 4-1. The first eluent composition was MeOH/ACN/HOAc/TEA 66.4/32.0/1.2/0.4 and it was diluted consecutively with MeOH/ACN 67.5/32.5. By this, the HOAc/TEA ratio was kept at $3X/X$, where X was varied by from 0.4 to 0.006 25% (for practical reasons, we

(22) Sajonz, P.; Yun, T.; Zhong, G.; Fornstedt, T.; Guiochon, G. *J. Chromatogr., A* **1996**, *734*, 75−81.

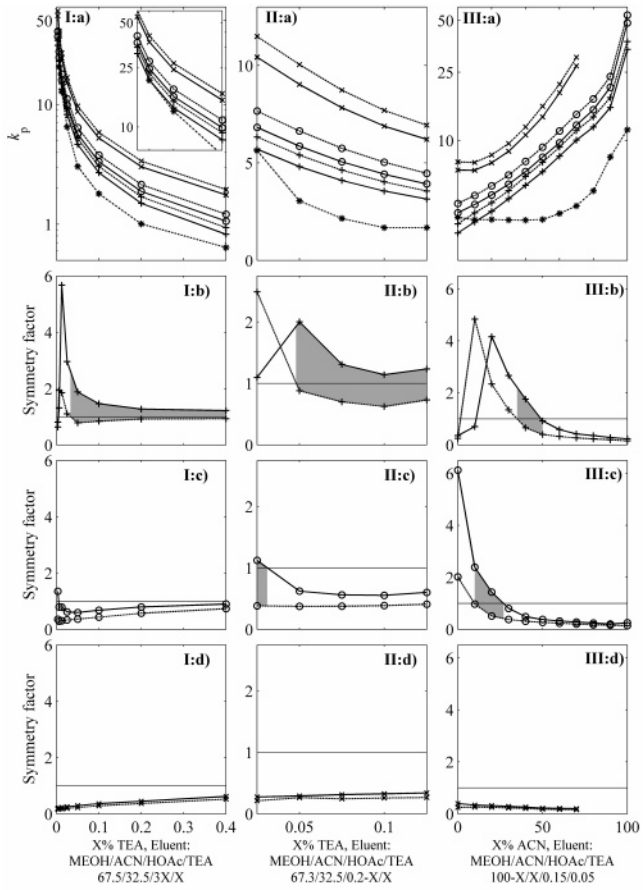

Figure 4. Capacity ratios and peak symmetries for different eluent compositions. Eluents, MeOH/ACN/HOAc/TEA: (I) 67.3/32.5/3*X*/*X*, (II) 67.3/32.5/0.2-*X*/*X*, and (III) 100-*X*/*X*/0.15/0.05. (a) Apparent capacity ratios (k_p) of perturbation (∗), alprenolol (+), propranolol (o), and atenolol (x); peak symmetries of (b) alprenolol, (c) propranolol, and (d) atenolol enantiomers. The solid lines are the *S*-enantiomers, dashed lines the *R*-enantiomers. Gray regions indicate opposite tailing; i.e., the first peak is anti-Langmuirian, the second is Langmuirian.

write the composition MeOH/ACN/HOAc/TEA 67.5/32.5/3*X*/*X*). In Figure 4-Ia, the apparent capacity ratios of the perturbation and solute peaks are displayed as a function of additive concentration, analogous to the situation depicted in Figure 1. As expected, the retention of the perturbation peak and all solutes decrease with increasing additive plateau concentration, due to increased competition for the stationary-phase surface. The TEA perturbation peak retention dependence on the plateau concentration is stronger than that for the solutes, as expected from eqs 3 and 4. For most eluents used, $\alpha_{p,i} < 1$ for all i, but a reversal of elution order between the perturbation peak and alprenolol takes place at very low additive concentration. The additive level was not decreased further since the retention times became very long and also because the pH stability became questionable (HOAc and TEA give pH buffering). The symmetry factors of the enantiomer peaks are shown in Figure 4-Ib−d. The symmetries change only little as the additive concentration is varied, except at very low additive levels and then only for the most weakly retained components. The peak symmetries are very unstable in situations where the perturbation and analyte peaks elute close to each other ($\alpha_{p,i} \approx 1$). A similar behavior is expected at very high additive levels, when all peaks elute close to t_0, but this was not verified. Apart from at the extremes, it can be seen that the (*S*)-alprenolol peak is always anti-Langmuirian and the (*R*)-alprenolol peak is always Langmuirian, at least for 5.0 mM samples (however, we will see later that the peak symmetry can change at high overload). This is the desirable situation with opposite tailing. This important section of the plot has been shadowed, and we will use the same highlighting throughout whenever we run into conditions yielding opposite tailing. The propranolol and atenolol enantiomer peaks are Langmuirian, and no change of total additive concentration can be made to achieve opposite tailing. This is in line with our hypothesis that TEA causes the deformations, as changes of the TEA plateau ideally cannot change the initial slopes of the adsorption isotherms. Symmetry changes should therefore only be observed when $\alpha_{0,i} > 1$ and $\alpha_{p,i}$ changes from above to below unity.

Next, the additive ratio was varied, whereas the MeOH and ACN concentrations were kept constant. In Figure 4-IIa−d are the measured apparent capacity ratios and peak symmetry factors obtained from eluents with composition MeOH/ACN/HOAc/TEA 67.3/32.5/0.2-*X*/*X*. Here, *X* was varied between 0.025 and 0.125%, limited by the pH stability range of the stationary phase. It should be noted that both pH and ionic strength are varied. Also, here the retention decreases with increased TEA concentration, and the peak symmetry is unstable if the additive perturbation and solute peak elute close to each other ($\alpha_{p,i} \approx 1$). Otherwise, the peak symmetry is affected little by the additive ratio.

Finally, the MeOH/ACN ratio was varied, while the HOAc and TEA concentrations were kept constant. In Figure 4-IIIa−d are the measured capacity ratios and peak symmetry factors obtained from eluents with composition MeOH/ACN/HOAc/TEA 100-*X*/*X*/0.15/0.05. Here, *X* was varied between 0 and 100%. The solute capacity ratios increase very rapidly with the ACN concentration. The apparent $k_{p,a}$ of the additive perturbation shows much smaller dependence; in fact, it remains almost constant from 0 to 50% ACN before it starts to increase significantly. This is a very important observation since it shows that the solutes respond differently to the MeOH/ACN ratio than the TEA additive does, indicating that β-blocker adsorption isotherms can be tuned in relation to the TEA adsorption isotherm by changes of eluent polarity. As can be seen in Figure 4-IIIb−d, the ACN concentration of the eluent has a dramatic impact on the peak symmetries. Both alprenolol and propranolol enantiomer peak shapes can be extensively tuned by altering the ACN concentration. At ACN levels below ~15%, alprenolol enantiomers elute very close to the perturbation peak ($\alpha_{p,i} \approx 1$), and the symmetries are unstable. Beyond this unstable region, $\alpha_{p,i} < 1$ and both alprenolol enantiomer peaks are initially anti-Langmuirian. When the ACN concentration is between 35 and 50%, the peaks will exhibit opposite tailing, whereas both peaks will be Langmuirian at ACN concentrations exceeding 50%. The same tuneability pattern holds for propranolol, although the ACN concentration must be lower, within 10 and 27%, to obtain opposite tailing. The atenolol enantiomer peaks, though, remain Langmuirian regardless of the ACN level.

Peak Shape Tuneability. The results above suggest that the TEA additive is strongly adsorbed and that it causes the observed solute peak deformations. The peak shapes are very tunable since the adsorption of additive and analytes respond differently to eluent polarity. Alprenolol and propranolol elution profiles corre-

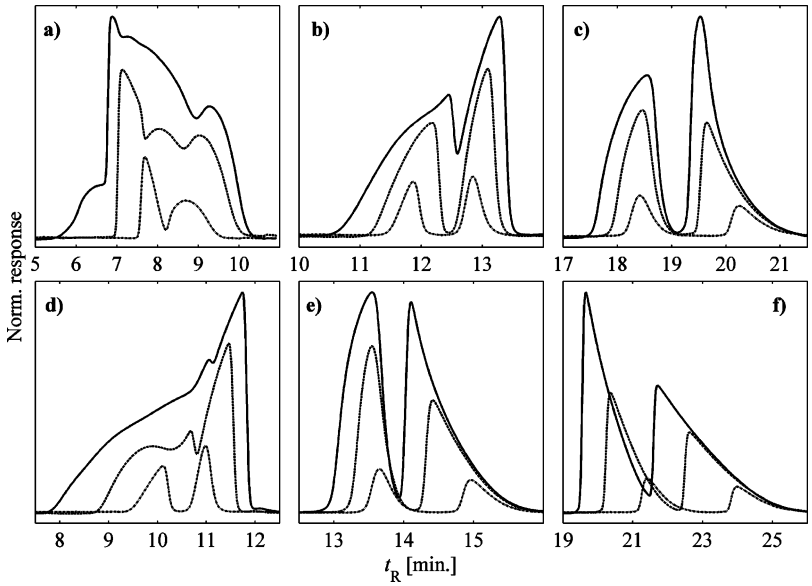

Figure 5. Peak shape tuneability of (a−c) alprenolol and (d−f) propranolol. Eluents: (a, d) MeOH/ACN/HOAc/TEA 99.8/0/0.15/0.05, (b, e) 67.3/32.5/0.15/0.05, and (c, f) 39.8/60/0.15/0.05. 50-μL injections of 5, 25, and 50 mM samples.

sponding to three different MeOH/ACN ratios are shown in Figure 5, illustrating the peak shape tuneability of these solutes; atenolol was left out since it is not tuneable. The eluents used were MeOH/ACN/HOAc/TEA (a, d) 99.8/0/0.15/0.05, (b, e) 67.3/32.5/0.15/0.05, and (c, f) 39.8/60/0.15/0.05. The injected concentrations were 5, 25 and 50 mM (sum of enantiomers) of either alprenolol (a−c) or propranolol (d−f), and the injected volume was 50 μL. With the first eluent, the perturbation peak (as measured by RI; not shown) elutes very close to the solutes ($t_{R,\,a} = 9.88$ min), so the solute shapes are deformed to different extent. The peak shapes are much more distinct with the other two eluents, since $\alpha_{p\ ,i} \ll 1$. The solute peak symmetries are strongly dependent on the MeOH/ACN ratio, but also on the sample size. As the sample size increases, both solute competition and the system perturbation increase. The solute bands become wider and may be torn between different velocity gradients corresponding to the perturbation peak and coherent disturbances. This observation is in line with previous reports.[13,14]

We know from the rule of thumb from the theoretical section that the solute peak symmetry depends on (i) the initial slope of the additive and solute adsorption isotherms (or equivalently $\alpha_{0\ ,i}$) and (ii) the elution order of solute and perturbation peaks on the additive plateau (or equivalently $\alpha_{p,\,i}$). These shifts are, however, very dramatic; the corresponding peaks are elongated and very deformed. Systems in which the perturbation peak elutes too close to the solutes ($\alpha_{p,\,i} \approx 1$) are the peaks elongated and very deformed (Figure 5a, d) and, therefore, not suitable for preparative separations. However, for most eluents used in Figure 4, the perturbation peak elutes long before the solutes ($\alpha_{p,\,i} \ll 1$). Also, in this section of the plots, symmetry inversion occurs. Here the cause should be changes of the initial slopes of the adsorption isotherms. In the case where the additive perturbation elutes before two enantiomer peaks do, according to theory, there are three possible outcomes: If the initial slope of additive adsorption isotherm is less steep than for both enantiomers ($\alpha_{0,\,S} < 1$, $\alpha_{0,\,R} < 1$), both analyte peaks will be Langmuirian at overload. If the initial slope of the additive adsorption isotherm is steeper than for both enantiomers ($\alpha_{0,\,S} > 1$, $\alpha_{0,\,R} > 1$), both analyte peaks will be anti-Langmuirian at overload. Finally, if the initial slope of the additive adsorption isotherm lies somewhere in between those of the enantiomers ($\alpha_{0,\,S} > 1$, $\alpha_{0,\,R} < 1$), the enantiomers' peaks will exhibit opposite tailing. It is obvious that the MeOH/ACN ratio is an important tool for tuning shapes probably because it affects α_0; this is going to be confirmed below by using the inverse method to estimate parameters for both the solutes and TEA. The size of the sample affects the peak symmetry in a way that cannot be quantified as easily, which might sometimes complicate the application of the rule of thumb.[13,14]

Table 1

(a) MeOH/ACN/HOAc/TEA 67.3/32.5/0.15/0.05

compd	a_I	b_I	a_{II}	b_{II}	α_0
TEA	22.2	113	7.88	101	
S-Alpr	8.99	43.6	13.8	54.0	1.32
R-Alpr			16.4	96.2	1.19
S-Propr	10.7	47.6	17.0	120.0	1.09
R-Propr			20.5	230	0.97
S-Aten	14.8	1.22	27.4	454	0.71
R-Aten			31.9	550	0.64

(b) MeOH/ACN/HOAc/TEA 39.8/60/0.15/0.05

TEA	41.9	146	10.5	89.5	
S-Alpr	21.7	21	18.7	101	1.30
R-Alpr			23.5	368	1.16
S-Propr	22.6	8.9	25.9	409	1.08
R-Propr			32.3	552	0.95
S-Aten	36.7	2.41	53.8	1220	0.58
R-Aten			63.3	1440	0.52

Adsorption Isotherm Estimation. The IM was used to estimate the adsorption isotherms of additive and solutes for the MeOH/ACN/HOAc/TEA 67.3/32.5/0.15/0.05 eluent. We considered several complex adsorption models, for instance, electrostatic ones, but the extreme run times were discouraging. We obtained good fit with the bi-Langmuir model, eq 10, so we decided not to increase the model complexity further. The best

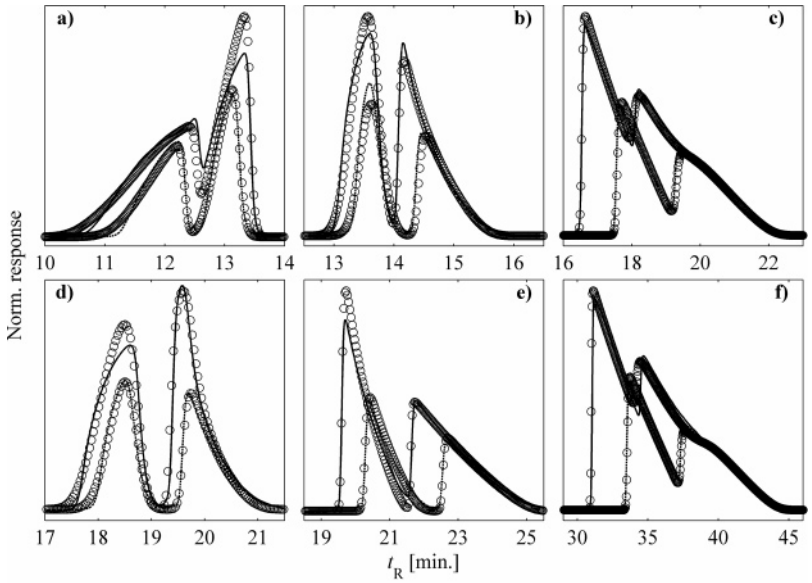

Figure 6. Overlay of experimental (lines) and simulated (symbols) elution profiles of (a, d) alprenolol, (b, e) propranolol, and (c, f) atenolol for two different eluents. Elution profiles corresponding to 50 μL of 25 and 50 mM sample injections used in the IM parameter fitting. (a–c) Eluent MeOH/ACN/HOAc/TEA 67.3/32.5/0.15/0.05), bi-Langmuir parameters from Table 1a. (d–f) Eluent MeOH/ACN/HOAc/TEA 39.8/60/0.15/0.05), bi-Langmuir parameters from Table 1b.

bi-Langmuir parameters and $\alpha_{0,i}$ values are shown in Table 1a. The initial slope of each adsorption isotherm is equal to the sum of the corresponding *a*-parameters, and so $\alpha_{0,i}$ were calculated from these slopes using eq 8. If the additive perturbation elutes before the solutes, the solute peaks should be Langmuirian for $\alpha_{0,i} < 1$ and anti-Langmuirian for $\alpha_{0,i} > 1$. From the parameters in Table 1, we would therefore expect anti-Langmuirian alprenolol peaks, Langmuirian atenolol peaks, and opposite tailing propranolol peaks. This is in agreement with the experimental profiles. One can also see in Table 1 that $\alpha_{0,i} \ll 1$ for the atenolol enantiomers, which indicates why the corresponding profiles show no tuneability; a very large shift in $\alpha_{0,i}$ is required to obtain opposite tailing and changes in MeOH/ACN cannot introduce such a large shift.

Figure 6a–c shows an overlay of experimental profiles (lines) and simulations (symbols) based on the fitted parameters of (a) alprenolol, (b) propranolol, and (c) atenolol. The profiles are the ones used in the fitting: 50 μL, 25 and 50 mM (5.0 mM profiles were also used in the fitting, but they were excluded from the figure for visual clarity). The model agreement is very convincing.

The IM fitting procedure was repeated with a MeOH/ACN/HOAc/TEA 39.8/60/0.15/0.05 eluent. The corresponding profiles are shown in Figure 6d–f; also, here the model agreement is very good. The bi-Langmuir parameters are displayed in Table 1b. Interestingly, the rule of thumb does not seem to apply perfectly in this case; the $\alpha_{0,i}$ for (*R*)-alprenolol and (*S*)-propranolol imply anti-Langmuirian peak shapes, whereas the experimental and simulated profiles are clearly Langmuirian (Figure 5c, f and Figure 6d, e). This disagreement could possibly be because the empirical rule was developed for a homogeneous model, whereas adsorption in the present study is clearly heterogeneous.

The parameters in Table 1a were also used to predict the elution profiles corresponding to two extreme injections. Figure 7 shows the experimental (lines) and simulated, predicted (symbols) profiles corresponding to (a, c) 50 μL of 100 mM and (b, d) 500 μL of 25 mM propranolol injections. UV detection (a, b) was used to measure the β-blocker peaks, whereas RI detection (c, d) was used to measure the perturbation peak. It should be noted that these experimental profiles were not used in the fitting, i.e., in the determination of the parameters in Table 1a. Although both the buffer capacity and the highest concentration used in the fitting are exceeded, the overlap is quite satisfactory. The simulations deviate some from the experimental profiles, but all the important attributes are properly predicted. The quality of the TEA perturbation fit (RI trace) is relatively low, but this is not surprising since the TEA adsorption isotherm parameters were estimated implicitly. Fractions were taken every 6 s during the elution of the perturbation peaks, and pH was measured after diluting with 600 μL of water. In Figure 7c and dm the pH is shown

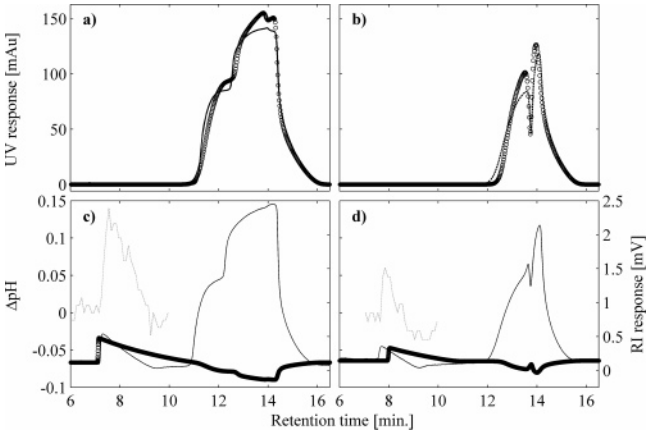

Figure 7. Overlay of experimental (lines) and simulated (symbols) elution profiles. Prediction of extreme profiles, corresponding to (a, c) 50 μL of 100 mM and (b, d) 500 μL of 25 mM propranolol samples. The propranolol profiles are best detected by UV (a, b), whereas the additive perturbation peak is best detected by RI (c, d). The effluent pH (dotted lines) rises during the elution of the additive perturbation. Eluent MeOH/ACN/HOAc/TEA 67.3/32.5/0.15/0.05, bi-Langmuir parameters from Table 1a.

Table 2

	MeOH/ACN/HOAc/TEA							
	79.8/20/0.15/0.05				67.3/32.5/0.15/0.05			
	$t_{R,1}$	Sym_1	$t_{R,2}$	Sym_2	$t_{R,1}$	Sym_1	$t_{R,2}$	Sym_2
acebutolol	12.61	1.01	13.02	0.24	14	0.24	14.7	0.17
clomipramin	13.31	0.14			14	0.31		
imipramin	13.75	0.1			14.25	0.77		
metoprolol HCl	11.65	4.93	12.42	2.22	13	2.89	13.67	0.35
metoprolol succinate	11.6	5.58	12.38	2.44	12.95	3.33	13.63	0.4
naphtylethylamine	12.66	0.51			14.32	0.1		
orphenadrine	12.31	10.48			12.83	12.52		
prilocaine	6.5	0.02			6.37	0.03	10.88	24.1
pyrrolidinyl norephedrine	11.8	5.87	12.7	0.65	13.11	3.71	14.06	0.19
quinidine	24.52	0.12			26.23	0.06		

to rise during the elution of the perturbation peak, which is expected since TEA is a base.

Generality of Results. The chromatographic behavior presented above is not limited to the current choice of column and solutes. 2-Phenylbutyric acid has been shown to be affected in a similar way when separated on a Kromasil 100−5-TBB chiral column (Eka Chemicals, Bohus, Sweden) using an eluent composed of hexane/ethyl acetate 85/15 with 0.1% formic acid additive (Figure 1 in ref 23).

In Table 2, the retention times and peak symmetries of 10 compounds are presented for two different eluents and the Chirobiotic T column. The flow rate was 1.50 mL min^{-1}, injection volume 50 μL, and injection concentration 25 mM. These compounds represent a broad spectrum of solutes, yet not all are chiral. Both Langmuirian and anti-Langmuirian and other deformations were observed. It is also clear that the peak shapes are responsive to the choice of weak eluent composition, probably by affecting $\alpha_{0,i}$.

Pyrrolidinylephedrine exhibits opposite tailing for the MeOH/ACN/HOAc/TEA 67.3/32.5/0.15/0.05 eluent whereas the second peak tends more for an anti-Langmuirian shape with the MeOH/ACN/HOAc/TEA 79.8/20/0.15/0.05 eluent. Orphenadrine is anti-Langmuirian for both eluents, whereas, for instance, quinidine is Langmuirian. Both succinate and HCl forms of metoprolol were injected to confirm that peak shapes do not change with the counterion. The salt forms yielded almost identical peak shapes and retention although the metoprolol succinate enantiomer peaks were somewhat sharper. Opposite tailing was observed for the MeOH/ACN/HOAc/TEA 67.3/32.5/0.15/0.05 eluent whereas anti-Langmuir/anti-Langmuir peaks were observed for the MeOH/ACN/HOAc/TEA 67.3/32.5/0.15/0.05 eluent. Prilocaine was severely distorted using both eluents. This is very easily explained from the observation that it coelutes with the TEA perturbation peak. This corresponds to the case illustrated in Figure 1d ($\alpha_{0,i} > 1$, $\alpha_{p,i} \approx 1$). In fact, the achiral prilocaine was subjected to peak split when the MeOH/ACN/HOAc/TEA 67.3/32.5/0.15/0.05 eluent was used, giving the impression that there were two peaks: the first one strongly Langmuirian, the second one strongly anti-Langmuirian.

From these observations we can conclude that non-Langmuirian solute peaks caused by strongly adsorbed additives are likely to be encountered in many modern chiral systems. Special consideration should therefore be given to, when possible, tune the peaks in the way outlined in the present work.

CONCLUSIONS

Solute peaks may have non-Langmuirian shapes although the adsorption isotherms governing the system are convex (type-I) if there is a strongly adsorbed additive present. The fundamental conditions dictating the peak shapes in such systems were studied already ~15 years ago, and the experimental systems used to validate the theories were skillfully constructed to show the effects, by the use of structurally related solutes and additives. In the present study, we have shown that these theories can be applied on more realistic and relevant experimental systems: separations on modern chiral stationary phases in the polar organic mode.

Detailed characterization of such systems by adsorption isotherm determination is very difficult; classical methods such as frontal analysis, elution by characteristic points, and plateau methods may be difficult to use due to the presence of adsorbing additives. We used the IM to measure the competitive adsorption isotherms of the solutes and additive, and it was shown that our suggested model is valid.

We found that triethylamine additive is strongly adsorbed in the Chirobiotic T chiral column for typical MeOH/ACN/HOAc/TEA eluents. For different compositions, β-blocker peaks had either Langmuirian or anti-Langmuirian shapes. One important result was that the solute peak shapes were strongly affected by the MeOH/ACN ratio, probably because the initial slopes of additive and solute adsorption isotherms have different polarity dependence. By changing this ratio, it was possible to tune the initial slope of the additive in relation to those of the β-blockers. A very interesting situation arose when the additive isotherm had a higher initial slope than the first eluting enantiomer, but lower than the second enantiomer, and if the perturbation peak eluted before both enantiomer peaks. Then the solutes displayed "opposite tailing"; i.e., the first enantiomer peak was anti-Langmuirian and the second Langmuirian, with sharp sides in between. Baseline resolution could then be achieved at very high sample loads.

With this particular chiral LC system, and probably many others, the effects of the strongly adsorbed additive are indeed advantageous. By tuning the peak shapes into opposite tailing by eluent polarity (or by the choice of additive), and then tuning the retention times (with preserved peak symmetries) by additive concentration in the eluent, it should be possible to obtain

(23) Lindholm, J.; Fornstedt, T. *J. Chromatogr., A* **2005**, *1095*, 50−59

conditions for very efficient preparative separations in terms of throughput and productivity. Utilization of opposite tailing for separations in batch and steady-state recycling[24] processes might be awarding, but a quantitative investigation of this is beyond the scope of this work.

ACKNOWLEDGMENT

This work was supported by grants from the Swedish National Graduate School of Scientific Computing (NGSSC) and the Swedish Research Council (VR). The Chirobiotic T column was a kind gift from Dr. Armstrong at Department of Chemistry and Biochemistry, University of Texas Arlington.

GLOSSARY

a	adsorption isotherm parameter
b	adsorption isotherm parameter (M^{-1})
C	concentration in mobile phase (M)
F	column phase ratio
k	capacity ratio
q	concentration in stationary phase (M)
t_0	column holdup time (s)
t_R	retention time (s)

Greek letters

α_0	selectivity
α_p	selectivity on an additive concentration plateau

Subscripts

I	bi-Langmuir nonchiral site
II	bi-Langmuir chiral site
a	additive
i, j	component index
p	additive concentration plateau
R	*R*-enantiomer
S	*S*-enantiomer

Received for review December 8, 2006. Accepted May 16, 2007.

AC062330T

(24) Grill, C. M.; Miller, L. *J. Chromatogr., A* **1998**, *827*, 359−371